# Intelligent Distributed Generation and Storage Units for DC Microgrids—A New Concept on Cooperative Control Without Communications Beyond Droop Control

Nelson L. Diaz, Tomislav Dragičević, *Member, IEEE*, Juan C. Vasquez, *Member, IEEE*, and Josep M. Guerrero, *Senior Member, IEEE*

***Abstract*—Low voltage dc microgrids have been widely used for supplying critical loads, such as data centers and remote communication stations. Consequently, it is important to ensure redundancy and enough energy capacity in order to support possible increments in load consumption. This is achieved by means of expansion of the energy storage system by adding extra distributed energy storage units. However, using distributed energy storage units adds more challenges in microgrids control, since stored energy should be balanced in order to avoid deep discharge or over-charge in one of the energy storage units. Typically, voltage droop loops are used for interconnecting several different units in parallel to a microgrid. This paper proposes a new decentralized strategy based on fuzzy logic that ensures stored energy balance for a low voltage dc microgrid with distributed battery energy storage systems by modifying the virtual resistances of the droop controllers in accordance with the state of charge of each energy storage unit. Additionally, the virtual resistance is adjusted in order to reduce the voltage deviation at the common dc bus. The units are self-controlled by using local variables only, hence, the microgrid can operate without relying on communication systems. Hardware in the loop results show the feasibility of the proposed method.**

***Index Terms*—Cooperative control, dc microgrids, droop control, fuzzy logic.**

## I. Introduction

With the increasing use of renewable energy sources (RES), microgrids appear as a solution for integrating distributed energy resources (DER), loads and energy storage systems (ESS) as controllable entities, which may operate in grid-connected or even islanded mode, either in ac or dc configuration [1]. In fact, during recent years, the interest in studying dc microgrids has increased considerably, since dc microgrids do not have issues associated with synchronization, reactive power flows, harmonic currents, and dc/ac conversion losses, which are inherent in ac microgrids [2].

On the other hand, the intermittent nature of RES, added together with unpredictable load fluctuations, may cause instantaneous power unbalances that affect the operation of the microgrid. Hence, ESS are required to guarantee reliability, security and power stability. In this sense, it is desirable to have two or more distributed ESS for providing redundancy and more energy support [2], [3].

Also, it is very important to coordinate RES and ESS units in order to avoid that the power generated by RES may collapse the system when ESS are full and there is a power unbalance in the microgrid. In this sense, the RES may change their control strategy from maximum power point tracking (MPPT) to a control strategy for regulating the voltage on the dc common bus. Moreover, the most effective way of charging a battery is by means of a two stage procedure which involves two different control loops [4]. Given the above points, the operation of each RES and ESS in the microgrid should be accompanied by a decision-maker strategy in order to switch between controllers.

Apart from that, when a number of ESS exist in a microgrid, a coordination is required to ensure stored energy balance among the units, in order to avoid deep-discharge in one of the energy storage unit and over-charge in the others. Therefore, during the process of charging, it is desirable to prioritize the charge of the unit with the smallest state of charge (SoC), and similarly, during the process of discharging, the unit with the highest SoC should provide more power to the microgrid than the others in order to ensure stored energy balance [5], [6]. In other words, conventional control loops for current sharing at each energy storage unit, may be complemented with stored energy balance control systems.

Commonly, voltage droop control method has been used when, two or more units are connected in parallel to the dc bus through a dc/dc converter, in order to ensure a current sharing feature among the units [3], [7], [8]. Droop method or, in his dc version, virtual impedance ensures equal or proportional fixed current sharing. However, this is not the best solution when the power electronics converters are connected to different prime

Manuscript received August 16, 2013; accepted July 17, 2014. Date of publication August 8, 2014; date of current version September 5, 2014. Paper no. TSG-00670-2013.

N. L. Diaz is with the Department of Energy Technology, Aalborg University, Aalborg 9220, Denmark; and also with the Universidad Distrital José De Caldas, Bogota, Colombia (e-mail: nda@et.aau.dk; nldiaza@udistrital.edu.co).

T. Dragičević, J. C. Vasquez, and J. M. Guerrero are with the Department of Energy Technology, Aalborg University, Aalborg 9220, Denmark (e-mail: tdr@et.aau.dk; joz@et.aau.dk; juq@et.aau.dk).

Color versions of one or more of the figures in this paper are available online at http://ieeexplore.ieee.org.

Digital Object Identifier 10.1109/TSG.2014.2341740

movers, for instance: photovoltaic systems or wind-turbines, and energy storage systems, and particularly distributed battery sets with different SoC.

In [3] a good stored energy balance has been achieved, by adaptively adjusting the virtual resistance (VR) in droop controllers. However, a centralized supervisory control is used, and there is a single point of failure in the system. Additionally, the voltage regulation is not strongly guaranteed. Other authors have proposed algorithms for adjusting the battery current based on a constant coefficient, whenever differences are detected in the SoC among batteries [9]. However, centralized controllers are required and the use of a constant coefficient may cause slow approximation or oscillations around the equilibrium point. Besides, in [9] voltage deviation at the common dc bus is not taken into account. In [10] a strategy for adjusting the droop controller based on the SoC in a distributed ESS has been proposed. However, the strategy proposed in [10] only takes into account the case when the batteries are supplying power to the load. Additionally, in [2] a gain-scheduling control in aggregation with a centralized fuzzy controller has been proposed in order to achieve good voltage regulation and power sharing, as well as stored energy balance in a distributed ESS. The solution proposed in [2] uses the centralized fuzzy controller in order to modify the voltage reference for balancing the stored energy.

In this paper, a decentralized and modular strategy based on fuzzy logic is proposed for achieving good stored energy balance among several ESS. In particular, one of the main advantages of fuzzy logic controllers is that they can manage different control objectives simultaneously [11]. Therefore, the proposed fuzzy system adjusts the VR of the droop controllers in accordance with the SoC at each ESS. Meanwhile, the fuzzy inference system is able to adjusts the VR in accordance to the common dc bus voltage, in order to reduce the voltage deviation. Fuzzy logic control has been lately proposed for energy management of ESS in microgrids thanks to its simplicity in summarizing complex algorithms [5]. However, in [5] just a single battery is analyzed.

This paper is organized as follows. In Section II the configuration and operation of the microgrid under isolated operation mode is described. Section III shows the design and operations of the proposed fuzzy controllers. Section IV presents the results under different operation modes. The proposed method is tested in a low voltage microgrid under islanded operation. Hardware in the loop by using a dSPACE 1006 and the controldesk shows the effectiveness of the proposed method and its advantages in comparison to conventional methods. Finally, Section V presents conclusions and perspectives for future works.

## II. Configuration and Operation of the DC Microgrid

The dc microgrid under study is composed by two RES [PV panels, and wind turbine generator (WTG)], dc loads, and two banks of valve regulated lead-acid (VRLA) batteries, as shown in Fig. 1. The microgrid is basically formed around $48V_{dc}$ common bus, these kinds of low voltage microgrids

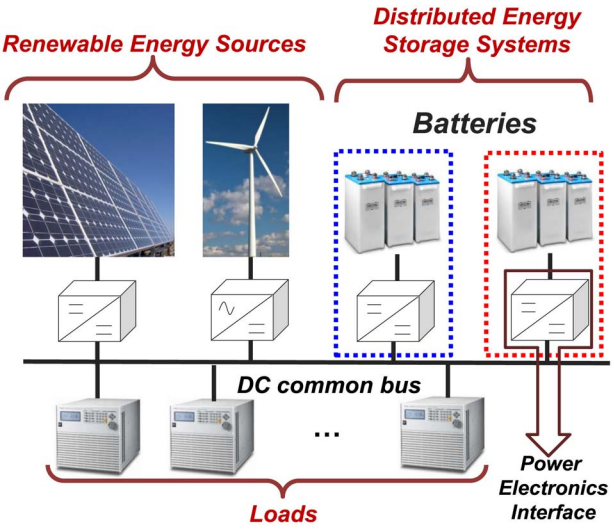


Fig. 1. DC microgrid configuration.

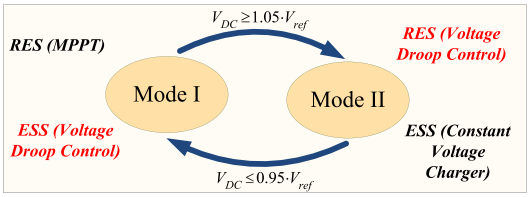


Fig. 2. Transition diagram between operation modes.

have been widely used for residential applications and for supplying energy to computer equipment in communication networks [12]–[14]. In particular, the microgrid will be analyzed under islanded operation mode since this mode is crucial for remote applications, and the interaction of batteries with RES plays an important role [15].

When the microgrid operates in islanded mode it is easy to identify two different operation modes based on the kind of distributed energy resource responsible of the dc common bus regulation (see Fig. 2). To be more precise, the dc common bus voltage can be regulated by distributed ESS (mode *I*) or by distributed RES (mode *II*).

Apart from that, the control strategy that governs each energy storage unit, changes in accordance to the SoC of the battery and the balance between the power generated by the RES and the power consumption. In the case of the RES, the control strategy changes in accordance to the voltage in the common dc bus in the same way that changes the operation mode of the microgrid [3], [16]. As a consequence, each DER, including batteries and RES, requires at least two inner control loops in order to operate under the two different operation modes and control states [3]. Fig. 3 shows a complete diagram of the microgrid with conventional inner control loops (fixed virtual resistance at the voltage droop controllers). In Fig. 3 it is also possible to see the block diagrams for the inner control loops used in the batteries converters (voltage droop control and constant voltage charger). Likewise, Fig. 3 shows the block diagrams for the inner control loops used at each RES converter (MPPT and voltage droop control). Fig. 4 shows the equivalent circuit under each operation mode, which will be explained in detail in this section.

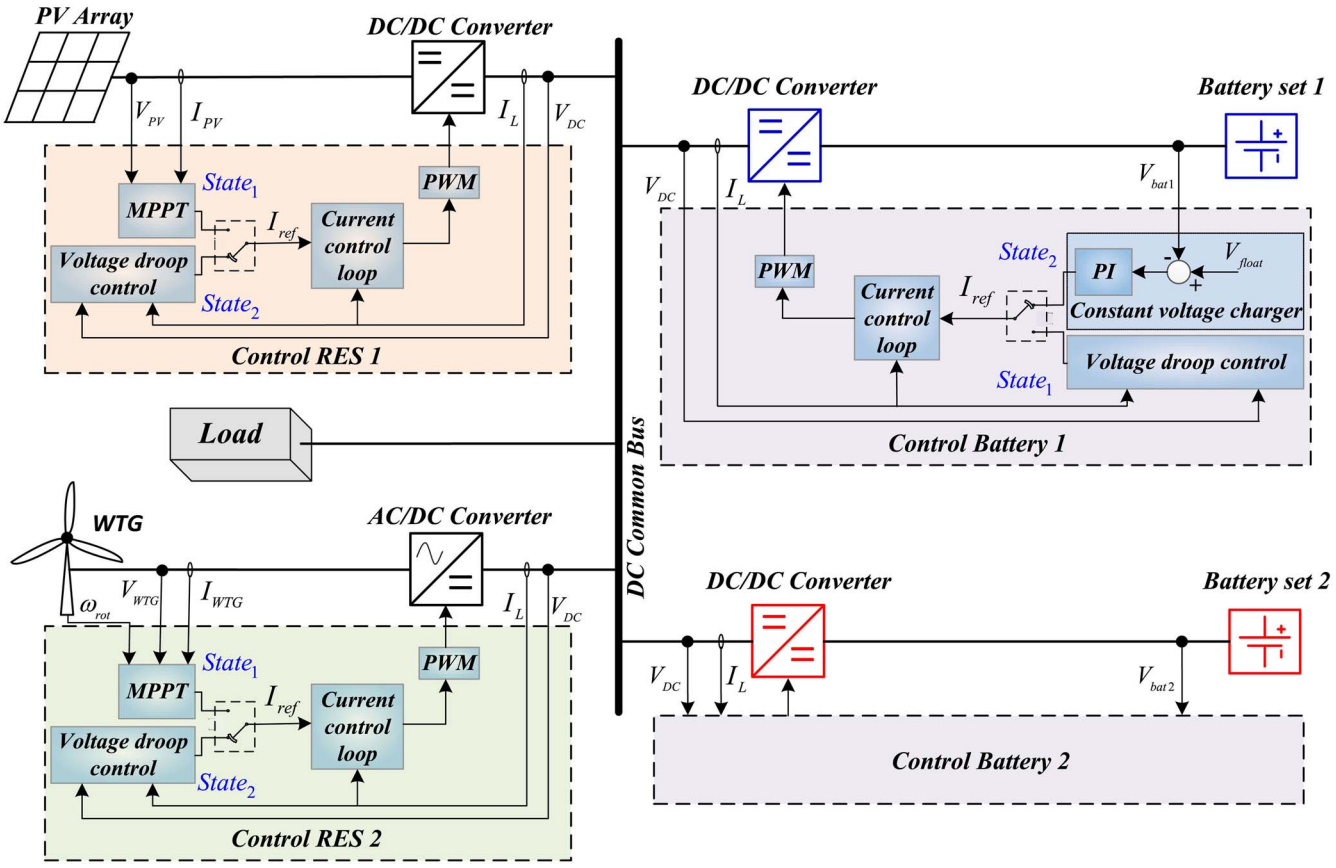


Fig. 3. Diagram of the dc microgrid with conventional inner control loops.

### A. Operation Mode I

In this operation mode, both RES operate under MPPT, and they can be seen as a constant power source (CPS) [17], [18]. Meanwhile, the converters of the batteries operate under voltage droop control and they are responsible of regulating the dc bus voltage. Fig. 4(a) shows the equivalent circuit under this operational mode in which a CPS is represented by a resistor in parallel to a constant current source, and the voltage source in series with the resistance ($Rd$) represents a battery operating under voltage droop control [3], [16].

Normally, under this operation mode the SoC of the batteries is maintained between 60% and 100%, the batteries will be charged or discharged depending on the power generated by RES and load consumption [9]. Then, a prolonged unbalance between available and consumed power will lead the batteries to deep-discharge levels (below 50%) [4]. At this point, it is important to implement proper schemes for load-shedding in order to avoid deeper discharge and reduce the battery lifetime [3], [9]. Load-shedding is out of the scope of this paper, but simple schemes based on voltage threshold can be seamlessly applied [19], [20]. On the contrary, when the power generated by RES is higher than load consumption, the batteries will be charged.

The most effective way of charging a VRLA battery is by a two stage procedure, current-limited followed by a constant voltage charger [3], [4]. During the first stage of charge, the current is limited by droop control loops. Subsequently, when the voltage per cell reach a value of $2.45 \pm 0.05$ volts/cell the voltage of the battery should be kept constant by the charger. This value is known as a float voltage ($V_{float}$). At this stage, the current at the battery will approach to zero asymptotically, and once it falls bellow a certain value, the battery may be considered as fully charged [4], [21].

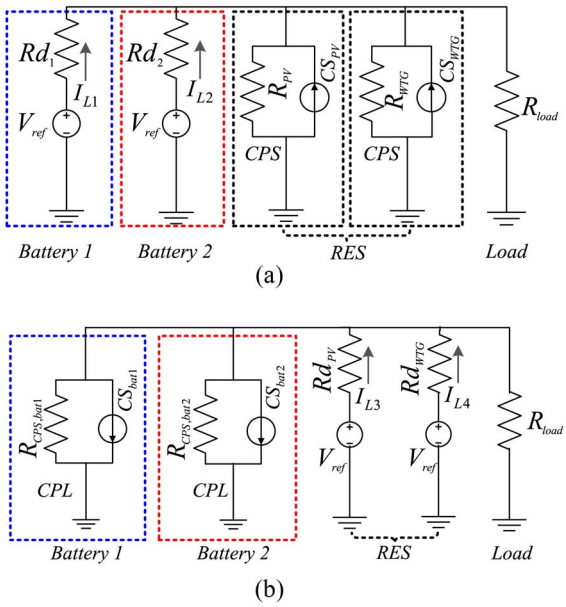


Fig. 4. Equivalent circuits of the proposed microgrid under (a) operation mode *I* and (b) operation mode *II*.

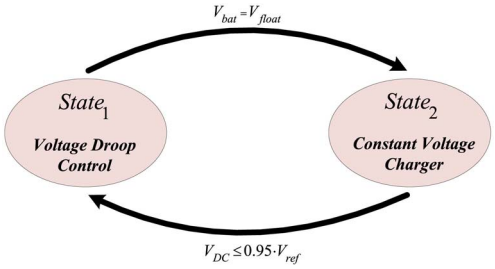


Fig. 5. Transition between inner control loops at each energy storage unit.

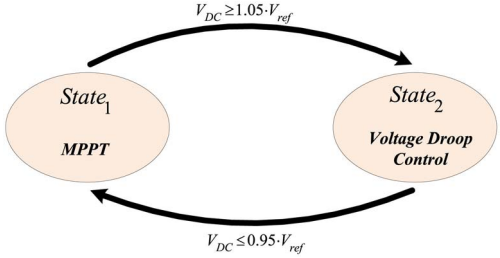


Fig. 6. Transition between inner control loops at each renewable energy source.

When the voltage of each battery reaches the reference value ($V_{float}$) the control of the converter switches to a constant voltage charger for the battery, in which, the battery draws as much current as needed to keep its voltage at $V_{float}$ [3]. When both batteries reach the float voltage, the RES continues operating in MPPT until a voltage threshold ($V_H = V_{ref} \cdot 1.05$) is reached in the dc bus. Then, the RES changes their inner control loops from MPPT to a voltage droop control in which the power drawn from the RES is limited to the power consumption of the microgrid. At this moment, the microgrid is under operation mode *II* [see Fig. 4(b)].

### B. Operation Mode II

In this mode, the RES are responsible for dc common bus regulation, since both batteries are under constant voltage charge. For that reason, the batteries will only take, as much current as necessary from the microgrid for keeping the batteries voltage regulated at ($V_{float}$). Then, batteries can be represented as constant power loads (CPL) [3], [22]. Fig. 4(b) shows the equivalent circuit under this operational mode.

The microgrid continues operating in this mode until a voltage threshold ($V_L = V_{ref} \cdot 0.95$) is reached at the dc bus. This may occur whether the consumption of the load is bigger than the power generated by the RES. At this point, the microgrid changes to operation mode *I*.

### C. Transition Between Controllers

For the transition between controllers, decentralized finite stated machines whit two states are used at each unit. In the case of the ESS, the transition from voltage droop control ($State_1$) to constant voltage charger ($State_2$) is decided by the battery voltage when $V_{bat} = V_{float}$. On the contrary, the transition from constant voltage charger ($State_2$) to voltage droop control ($State_1$) is decided by the voltage on the dc common bus when $V_{DC} \leq V_L$. Fig. 5 shows the finite state machine that represents the transition between inner control loops at each energy storage unit.

In the case of the RES, the transitions from MPPT ($State_1$) to voltage droop control ($State_2$) and from voltage droop control ($State_2$) to MPPT ($State_1$) are decided by the voltage on the dc common bus, when $V_{DC} \geq V_H$ and $V_{DC} \leq V_L$ respectively. Note that the transitions defined for the inner control loops at RES are basically the same defined for microgrid operation modes. It is important to say that smooth transitions between control loops, is achieved by means of enforcing initial conditions of inactive PI controller to the value of the output of the active one [3]. Fig. 6 shows the finite state machine that represents the transition between controllers at each renewable energy source. The following sections, will be focused on explaining the operation of the voltage droop controllers and the fuzzy adjustment of the virtual resistance.

## III. Fuzzy Adjustment of the Virtual Resistance

The main objective behind the design of fuzzy systems for adjusting virtual resistances, is ensuring stored energy balance among distributed energy storage units, and consequently avoid deep discharge in one of the batteries. Apart from that, another control objective is added into the fuzzy system in order to reduce the voltage deviation in the common dc bus. Finally, the proposed strategy is designed to be decentralized, since only local variables are to be used for performing the adjustment of the virtual resistances. Taking into account that voltage droop controllers are used by ESS and RES at different operational modes of the microgrid, a different fuzzy controller may be designed for ESS and for DER.

### A. Fuzzy Adjustment for Battery Charge and Discharge

When batteries are in the process of charge and discharge, the power balance is managed by droop control loops [3]. Therefore, the output voltage is given by the following equation:

$$V_{DC} = V_{ref} - I_{Li} \cdot Rd_i \tag{1}$$

where $Rd_i$ is the virtual resistance at each droop control loop, $V_{DC}$ is the voltage at the common dc bus, $V_{ref}$ is the voltage reference of the common dc bus, and $I_{Li}$ is the output current at each converter. In consequence, the battery with the lowest *Rd* will inject/extract more current in order to keep the power balance in the microgrid [23]. For that reason, the battery with the lowest *Rd* will be charged or discharged faster than the other.

In light of the above, it is desired that the battery with the lowest SoC is charged faster than all the others for ensuring stored energy balance. Then, a smaller *Rd* should be assigned to that battery. Likewise, when batteries are supplying the microgrid, it is desired that a bigger *Rd* is assigned to the battery with the lowest SoC, in order to prevent a deep discharge and balance the stored energy.

What is more, to prevent high voltage deviation at the dc bus, a smaller value for *Rd* is desirable when ($V_{DC}$) is far from $V_{ref}$. On the contrary, when the voltage at the dc bus $V_{DC}$ is near to $V_{ref}$ it is expected the highest value for *Rd*.

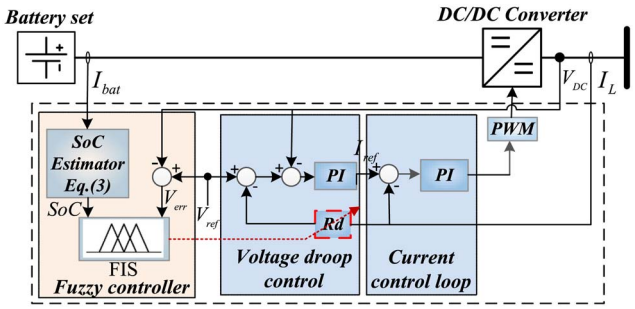


Fig. 7. Control diagram of the proposed fuzzy-based virtual resistance for ESS under operation mode *I*.

In particular, a fuzzy inference system (FIS) can easily summarize all the qualitative knowledge, expressed above. Indeed, a fuzzy controller can easily deal with different control objectives at the same time which are, in this particular case, stored energy balance and dc bus voltage deviation. In other words, a fuzzy inference system can use the experience and the knowledge of an expert about the expected behavior of the system in order to work out the virtual resistance at each control loop.

Given the above points, a Mamdani FIS has been proposed for adjusting the resistance *Rd* at each battery-converter system [24]. The FIS uses the SoC and the voltage error ($V_{err}$) expressed in (2) as the inputs, and the VR *Rd* as the output. The SoC is estimated by ampere-hour (Ah) counting method expressed in (3)

$$V_{err} = V_{ref} - V_{DC} \tag{2}$$

$$\text{SoC} = \text{SoC}(0) - \int_0^t \frac{I_{bat}(\tau)}{C_{bat}} d\tau \tag{3}$$

where SoC(0) represents the initial SoC, $C_{bat}$ is the capacity of the battery and $I_{bat}$ is the current of the battery [4]. Fig. 7 shows the diagram of the fuzzy controller used for the adjustment of the virtual resistance *Rd*. To be more precise, the fuzzy control is only used under operation mode *I*, when the battery is under voltage droop control in $State_1$.

Fig. 8 shows the control surface of the proposed FIS, which summarizes the behavior of the fuzzy inference system, where, the virtual resistance is adjusted based on the expected behavior explained before.

To put it in another way, Fig. 9(a) and (b) shows the Fig. 8 split into two figures that represent the process of charge and discharge respectively. Fig. 9(a) and (b) makes evident that the voltage deviation takes an important role into the performance of the system that is why the FIS tries to reduce the voltage deviation but it does not try to eliminate the voltage deviation. Hence, bus signaling takes an important role in the performance of the system [16].

Furthermore, the range of the output (*Rd*) in the FIS can be established by analyzing the circuit in Fig. 4(a), where a general expression for a general number of ESS and RES operating in MPPT may be expressed as shown in the following equation:

$$V_{DC} = \frac{\frac{V_{ref}}{R_{deq}} + I_{\text{CPS}}}{\frac{1}{R_{deq}} + \frac{1}{R_{load}} + \frac{1}{R_{\text{CPS}}}} \tag{4}$$

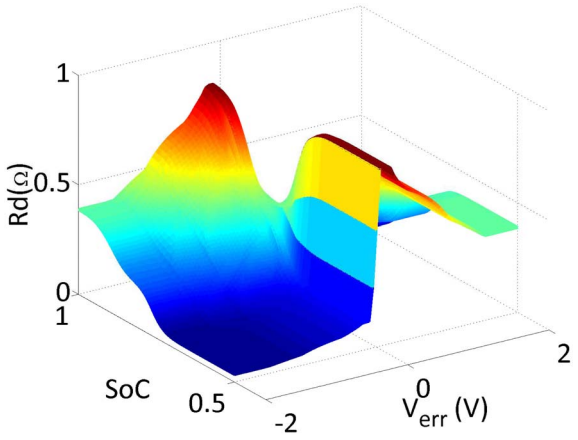


Fig. 8. Control surface of the fuzzy inference system.

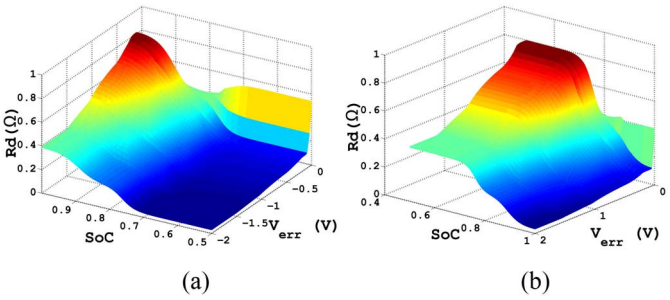


Fig. 9. Control surface under (a) process of charge and (b) process of discharge.

where $R_{deq}$ and $R_{\text{CPS}}$ are the equivalent VR and the equivalent resistant of the RES, seen as CPS, respectively [3]. $I_{\text{CPS}}$ is the equivalent current of the CPS. $R_{\text{CPS}}$ and $I_{\text{CPS}}$ can be well approximated by

$$R_{\text{CPS}} \approx \frac{V_{DC}^2}{P_{\text{CPS}}} \tag{5}$$

$$I_{\text{CPS}} \approx 2\frac{P_{\text{CPS}}}{V_{DC}} \tag{6}$$

where $P_{\text{CPS}}$ is the total power generated by RES. By replacing (5) and (6) in (4) it is possible to obtain the following equation:

$$V_{DC}\left(\frac{1}{R_{deq}} + \frac{1}{R_{load}}\right) - P_{\text{CPL}} - \frac{V_{ref}}{R_{deq}} = 0 \tag{7}$$

from (7) gives a solution for the common dc voltage

$$V_{DC} = \frac{\frac{V_{ref}}{R_{deq}} + \sqrt{\left(\frac{V_{ref}}{R_{deq}}\right)^2 + 4P_{\text{CPS}}\left(\frac{1}{R_{deq}} + \frac{1}{R_{load}}\right)}}{2\left(\frac{1}{R_{deq}} + \frac{1}{R_{load}}\right)} \tag{8}$$

where the value of the power generated by RES is taken as positive. Thus, just the positive solution is viable in this case, since the voltage of the common dc bus has to be positive. Then, when a maximum voltage deviation is defined, it is possible to solve (8) in order to determine the maximum and minimum value for *Rd*.

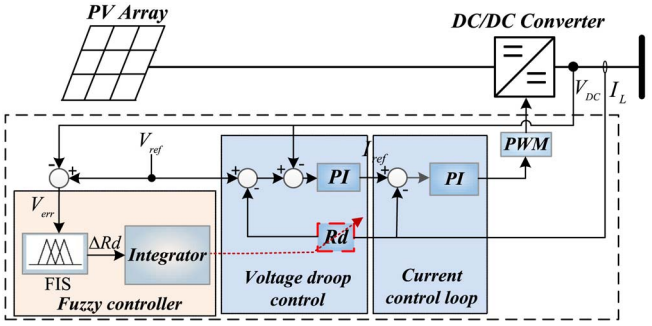


Fig. 10. Control diagram of the proposed fuzzy-based virtual resistance for RES under operation mode *II*.

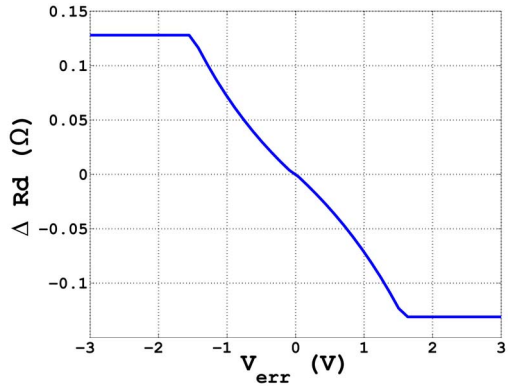


Fig. 11. Control surface $\Delta Rd$ versus $V_{err}$.

### B. Fuzzy Adjustment for Voltage Regulation Under Mode II

When the system operates under operation mode *II*, the RES are responsible for dc bus voltage regulation. At this point, both RES are operating under droop control loops ($State_2$), as can be seen in Fig. 3. Similarly, the virtual resistance $Rd$ at each unit can be adjusted for reducing the voltage deviation.

For that reason, an iterative adjustment of the virtual resistance has been proposed for obtaining good voltage regulation as well as good power sharing at the same time. The adjustment of $Rd$ is based on a fuzzy inference system of which output is an incremental signal ($\Delta Rd$). Then, depending on the voltage error ($V_{err} = V_{ref} - V_{DC}$), the virtual resistance will be increased or decreased. Fig. 10 shows the diagram of the control loop used for the adjustment of ($Rd$) at each RES unit. At this point, the microgrid is under operation mode *II* and the control loops are in $State_2$. The controller comprises a FIS and an integrator. Fig. 11 shows the control surface of the fuzzy inference system.

## IV. Hardware in the Loop Results

The performance of the microgrid using the proposed fuzzy methods has been tested in simulation by using a dSPACE 1006 and the controldesk. The performance is also compared with a microgrid in which a fixed virtual resistance ($Rd_{nom}$) is used in the droop control loop. Table I summarizes the main parameters of the system.

The first comparison in the performance of the system is shown in Figs. 12 and 13 with fixed VR value and with fuzzy adjustment of the VR respectively. An initial SoC of 75% for battery 1 (*bat*1) and 58% for battery 2 (*bat*2) has been established. Each figure shows the voltage at the batteries, the SoC of battery 1 $SoC_{bat1}$ and the SoC of battery 2 $SoC_{bat2}$, the current at battery 1 $I_{bat1}$ and the current at battery 2 $I_{bat2}$, and finally the voltage in the dc common bus $V_{DC}$. The simulation time is split into four stages in order to indicate the behavior of the system clearly.

TABLE I
Parameters of the Microgrid

| Parameter | Symbol | Value |
|---|---|---|
| DC bus voltage reference | $V_{ref}$ | 48V |
| Maximum power from RES | $P_{max}$ RES | 300W |
| Maximum power in the load | $P_{Load_{max}}$ | 250W |
| Float voltage | $V_{float}$ | 54V |
| Nominal virtual resistance | $Rd_{nom}$ | 0.8Ω |
| Low voltage threshold | $V_L$ | 45.6V |
| High voltage threshold | $V_H$ | 50.4V |
| Nominal Battery Capacity | $C_{bat}$ | 0.02(Ah) |

During the first stage (T1), the microgrid is operating under mode *I*, combined RES generate 290W and the batteries are being charged. It can be seen that in the system that uses the fuzzy controllers (see Fig. 13) the SoC of battery 2 approaches the SoC of battery 1 asymptotically. At the end of T1, battery 1 reaches its float voltage, therefore, battery 1 changes its inner control loop from voltage droop control ($State_1$) to constant voltage charger ($State_2$). It is possible to see the voltage deviation is only incrementally smaller in the system with fuzzy controllers (less than 48.5V in Fig. 12). However, the priority at this point is to balance the stored energy.

During the second stage (T2), battery 2 reaches its float voltage ($V_{float}$). Hence, it changes its inner control lopp from ($State_1$) to ($State_2$). It is possible to see that despite battery 1 is charged faster at the beginning in the microgrid with fixed virtual resistance (see Fig. 12) the total time of charge of both batteries (T1+T2) is less in the system with fuzzy controllers (see Fig. 13), thanks to the approach in the SoC of both batteries.

During third stage (T3), both batteries are under constant voltage charge and the RES are still in MPPT control ($State_1$). At this point, the voltage in the dc bus ($V_{DC}$) increases. After a while, $V_{DC} = V_H$ and the system changes to operation mode *II* (T4). In the transition from T3 to T4 it is possible to see big spikes in the battery currents when the microgrid uses fixed virtual resistance (see Fig. 12). These big spikes are due to the fixed value in the virtual resistance. On the contrary, the microgrid with fuzzy adjustment of the virtual resistance (see Fig. 13), slows down the transition in the dc bus voltage and eliminates the big spikes in the current of the batteries.

During forth stage (T4), batteries are under constant voltage charge and RES are under voltage droop control ($State_2$). Then, the current that they draw decrease exponentially. At the same time, it can be seen that in the system with fuzzy controllers the voltage deviation is smaller than in the system with fixed virtual resistance. In short, it may be seen that by using the FIS it is possible to assure stored energy balance and additionally to reduce the output voltage deviation.

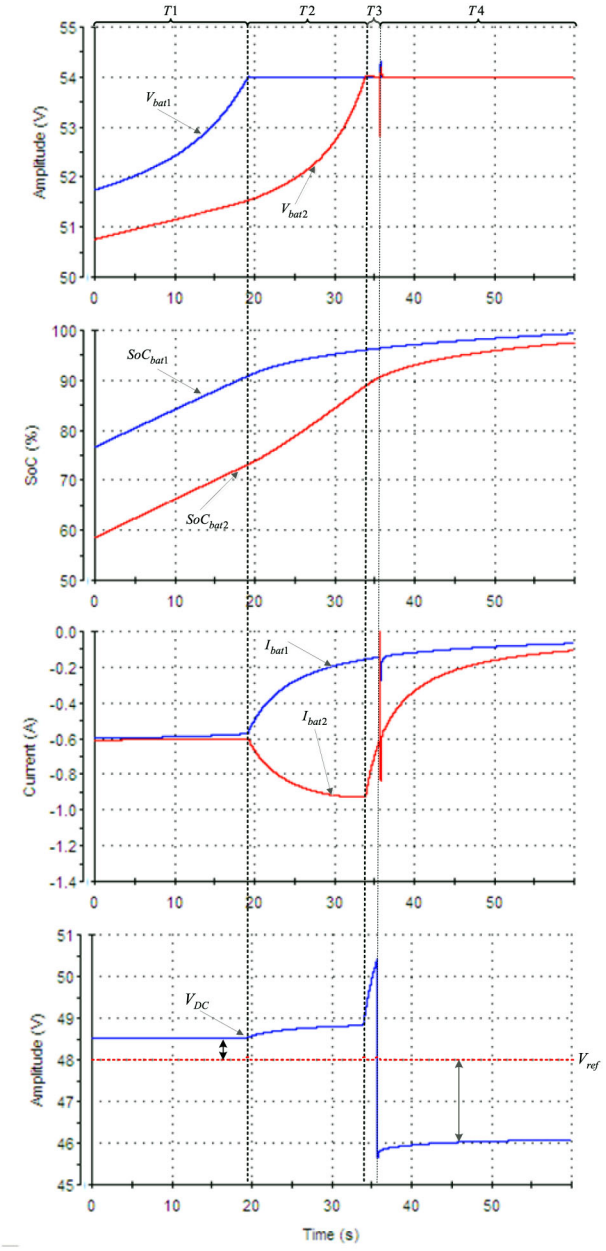


Fig. 12. Simulation result when the microgrid changes from operation mode *I* to operation mode *II* with fixed virtual resistance value at the inner control loops.

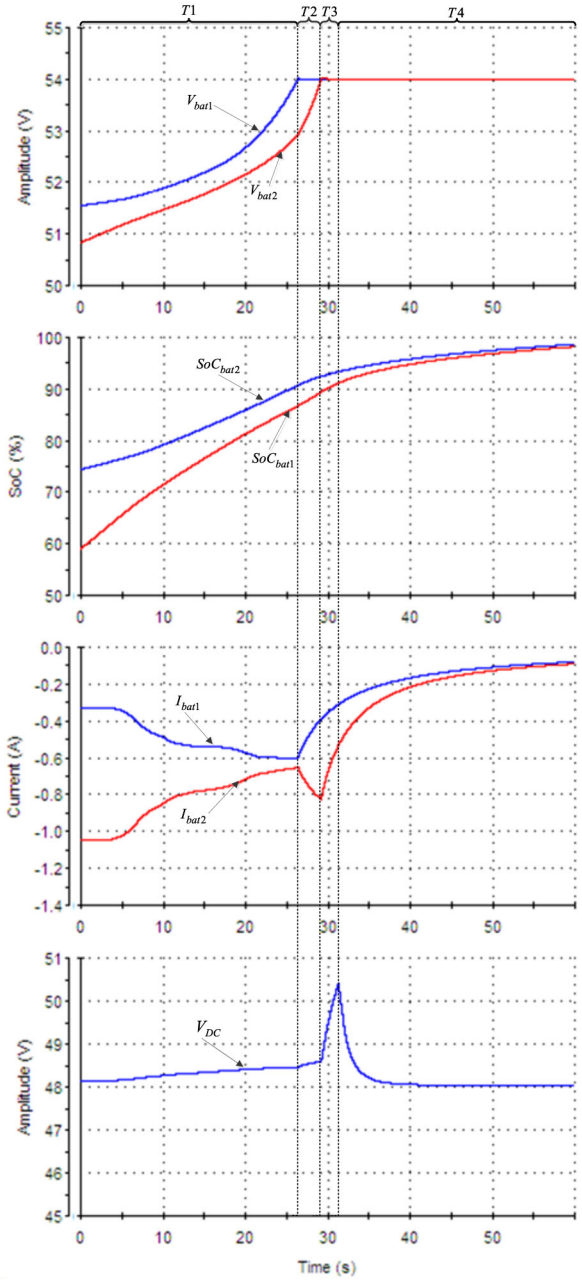


Fig. 13. Simulation result when the microgrid changes from operation mode *I* to operation mode *II* using the proposed fuzzy-based virtual resistance.

Figs. 14 and 15 show the performance of the microgrid when the power generated by RES varies during the time, with fixed virtual resistance value and with fuzzy adjustment of the VR respectively. Then, it is possible to see the performance of the proposed solution under charge and discharge of the batteries. In this scenario, the microgrid is operating under mode *I* mainly, and consequently, the inner control loop at each ESS and RES unit are in $State_1$ until the end of T3. Figs. 14 and 15 show the power generated by combined RES, the voltage at the batteries, the SoC at both batteries, the current at the batteries, and the voltage at the common dc bus.

To start with the analysis, during the first stage (T1) the power generated by combined RES is 300W. For that reason, both batteries are being charged, it may be seen in Fig. 15 that the SoC of battery 1 approaches the SoC of battery 2. On the other hand, in Fig. 14 it can be seen that the unbalance in the stored energy never changes.

During the second stage (T2), the power generated by RES is less than the load consumption (175W), therefore the batteries are discharged for supporting the unbalance between consumed and generated power. During T2, in Fig. 15 the unbalance in the stored energy is also reduced. On the other hand, in Fig. 14 the unbalance in the stored energy remains constant. At this point, it is important to say that if the batteries continues being discharged, battery 2 will be under deep discharge (below 60%). In fact, at the end of T2 in the microgrid with fuzzy controllers the charge of battery 2 is 18% higher than in the system without fuzzy controllers.

During third stage (T3), the power generated by RES is 275W, consequently the batteries will be charged until the

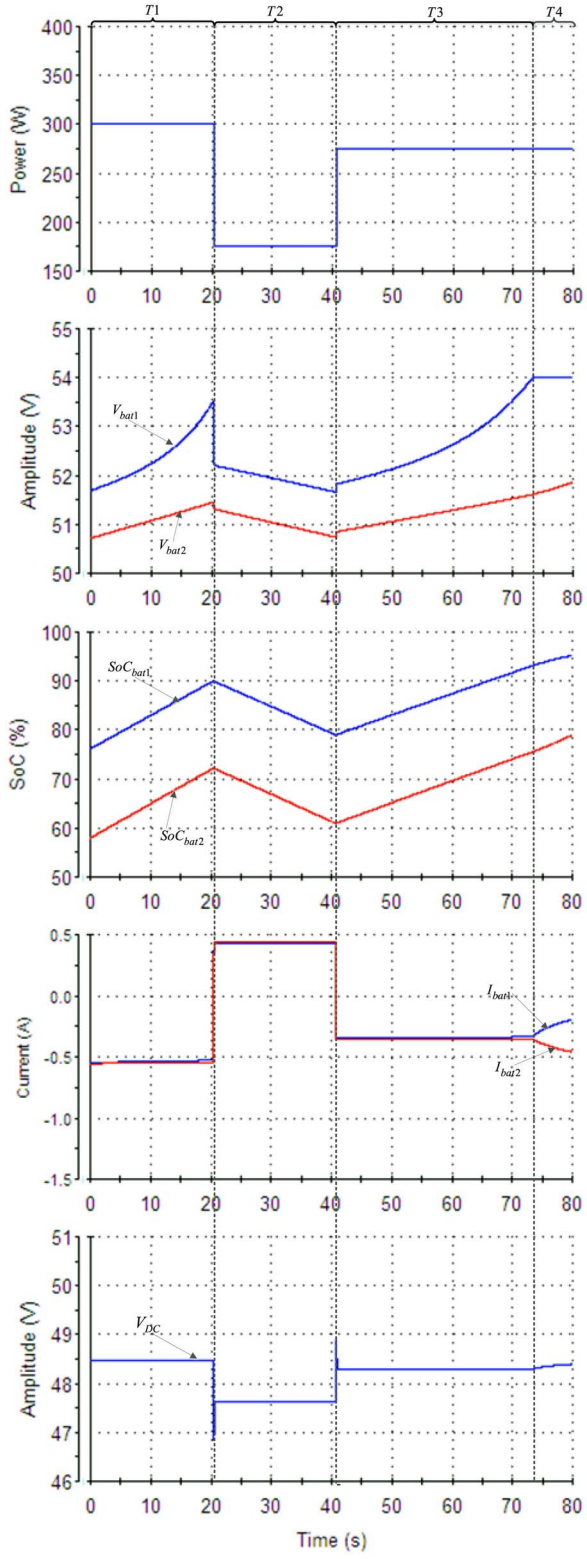


Fig. 14. Simulation results for showing the process of charge and discharge of batteries when the microgrid operates under mode *I* with fixed virtual resistance value.

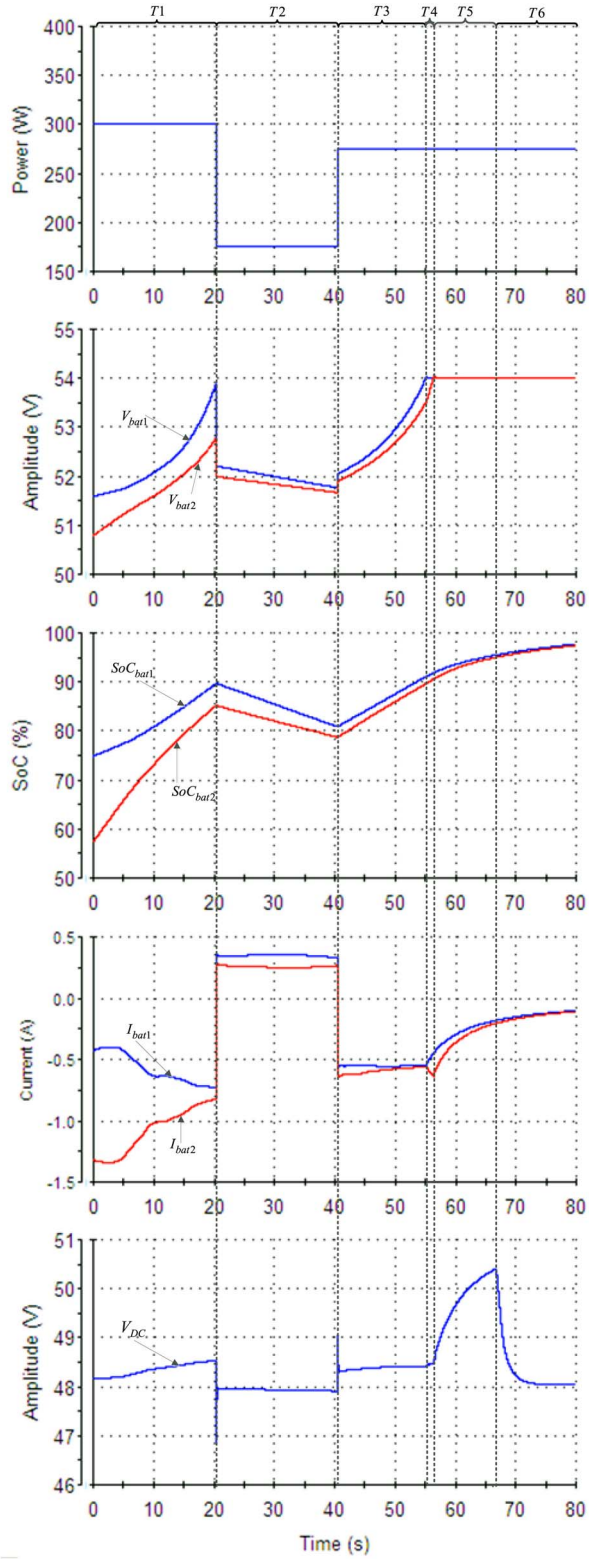


Fig. 15. Simulation results for showing the process of charge and discharge of batteries when the microgrid operates under mode *I* using the proposed fuzzy-based virtual resistance.

voltage of battery 1 reaches $V_{float}$. Since, the process of charge is faster with the fuzzy controllers, the transition to operation mode *II* (T4 + T5 + T6), can be seen in Fig. 15 but not in Fig. 14. The transition from operation mode *I* to operation mode *II* was explained in detail in Figs. 12 and 13. In fact, after T4 in Fig. 14 the response of the system is similar to the behavior shown in Fig. 12.

In Fig. 14 it is possible to see that the droop controllers ensures an equal current sharing for both batteries, when a

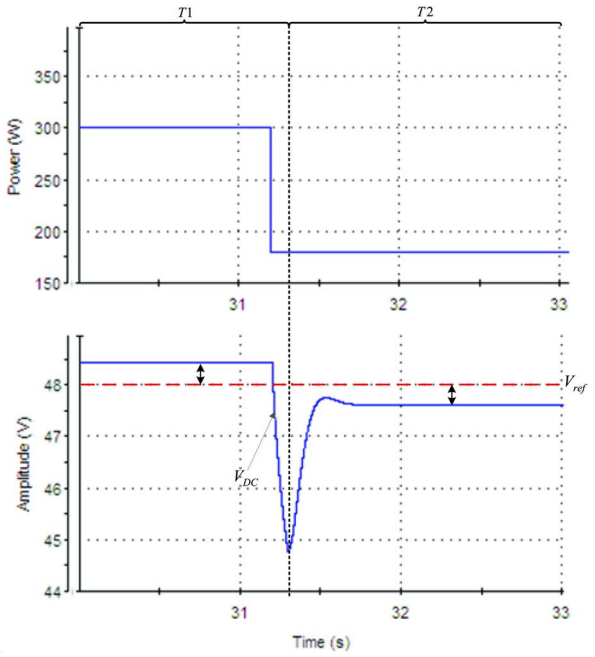


Fig. 16. Simulation results when the microgrid change from operation mode *II* to operation mode *I*, with fixed virtual resistance value.

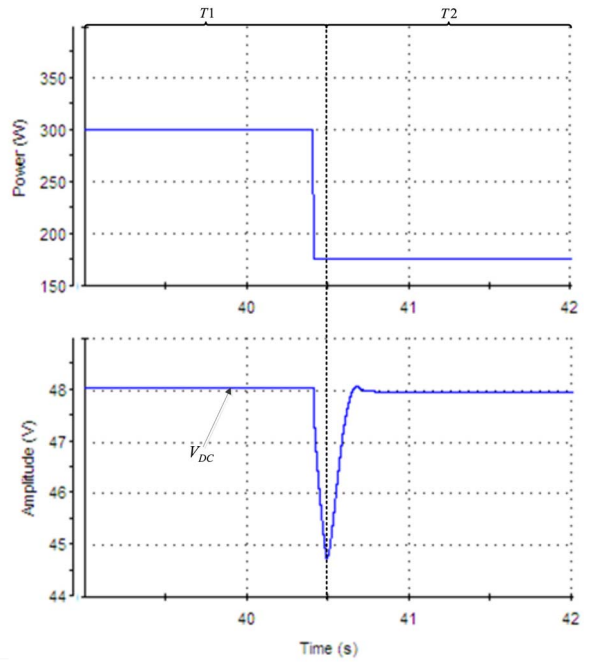


Fig. 17. Simulation results when the microgrid change from operation mode *II* to operation mode *I*, by using fuzzy controllers.

fixed virtual resistance is used. Meanwhile, In the case of using a fuzzy based-virtual resistance (see Fig. 15) the current sharing is decided by the SoC at each battery.

Finally, the last comparison is shown in Figs. 16 and 17. These figures show the behavior of the microgrid when it changes from operation mode *II* to operation mode *I*, with fixed virtual resistance and with fuzzy adjustment of the virtual resistance respectively.

In Figs. 16 and 17, during the first stage (T1), the batteries are under voltage regulation mode, and then, the dc bus is regulated by RES which operate under voltage droop control ($State_2$). Moreover, in T1 the batteries are almost full charged, and it can be assumed that both batteries have the same state of charge. For that reason, the current in the batteries is virtually the same. It is possible to see that the voltage regulation is considerably better in the response of the system which uses fuzzy controllers (see Fig. 17). Before the end of T1, a sudden drop in the power generated by RES (from 300W to 175W) causes a fall in the dc bus voltage. After a while, when the voltage in the dc bus is less than the voltage threshold $V_L$ the microgrid moves to operation mode *I*.

During the second stage (T2), in Figs. 16 and 17, the batteries are in charge of the regulation of the dc bus voltage, because of this, batteries are operating under voltage droop control ($State_1$), and the virtual resistance *Rd* is adjusted by means fuzzy controllers (see Fig. 17). On the contrary, Fig. 16 shows the response of the microgrid with fixed virtual resistance. It is possible to see that the voltage deviation is smaller when the fuzzy adjustment is used.

## V. Conclusion

The proposed adjustment of the virtual resistance by using a fuzzy inference system, assures good storage energy balance and low voltage deviation. Additionally, this strategy is absolutely modular, expandable, and it is not required a centralized control. As a matter of fact, it can be used directly when a new energy storage unit has to be added to the microgrid without any modification. Likewise, the proposed method shows a faster charge in the batteries compared to traditional methods. In addition, it is shown that the priority of the fuzzy controller is the stored energy balance, and once the stored energy balance is achieved, the fuzzy controller keeps regulating the voltage deviation. It is important to say that a steady state error is always desired in the dc bus, since the dc voltage is used for bus signaling.

In general, the FIS proposed in this paper has shown its advantages in dealing with different control objectives. Another advantage of the fuzzy controller is that the same FIS can be easily scaled to different values of *Rd*. On top of that, the microgrid can operate in a stable way under different scenarios without using communications.

## References

[1] T. Vandoorn, J. Vasquez, J. De Kooning, J. Guerrero, and L. Vandevelde, "Microgrids: Hierarchical control and an overview of the control and reserve management strategies," *IEEE Ind. Electron. Mag.*, vol. 7, no. 4, pp. 42–55, Dec. 2013.

[2] H. Kakigano, Y. Miura, and T. Ise, "Distribution voltage control for DC microgrids using fuzzy control and gain-scheduling technique," *IEEE Trans. Power Electron.*, vol. 28, no. 5, pp. 2246–2258, May 2013.

[3] T. Dragičević, J. Guerrero, J. Vasquez, and D. Skrlec, "Supervisory control of an adaptive-droop regulated DC microgrid with battery management capability," *IEEE Trans. Power Electron.*, vol. 29, no. 2, pp. 695–706, Feb. 2013.

[4] *IEEE Guide for Optimizing the Performance and Life of Lead-Acid Batteries in Remote Hybrid Power Systems*, IEEE Standard 1561-2007, pp. C1–C25, May 2008.

[5] Y.-K. Chen, Y.-C. Wu, C.-C. Song, and Y.-S. Chen, "Design and implementation of energy management system with fuzzy control for DC microgrid systems," *IEEE Trans. Power Electron.*, vol. 28, no. 4, pp. 1563–1570, Apr. 2013.
[6] J. Vasquez, J. Guerrero, M. Savaghebi, J. Eloy-Garcia, and R. Teodorescu, "Modeling, analysis, and design of stationary-reference-frame droop-controlled parallel three-phase voltage source inverters," *IEEE Trans. Ind. Electron.*, vol. 60, no. 4, pp. 1271–1280, Apr. 2013.
[7] P. Karlsson and J. Svensson, "DC bus voltage control for a distributed power system," *IEEE Trans. Power Electron.*, vol. 18, no. 6, pp. 1405–1412, Nov. 2003.
[8] J. Schonberger, R. Duke, and S. Round, "DC-bus signaling: A distributed control strategy for a hybrid renewable nanogrid," *IEEE Trans. Ind. Electron.*, vol. 53, no. 5, pp. 1453–1460, Oct. 2006.
[9] Y. Zhang, H. J. Jia, and L. Guo, "Energy management strategy of islanded microgrid based on power flow control," in *Proc. IEEE PES Innov. Smart Grid Technol. (ISGT)*, Washington, DC, USA, Jan. 2012, pp. 1–8.
[10] X. Lu *et al.*, "SoC-based droop method for distributed energy storage in DC microgrid applications," in *Proc. IEEE Int. Symp. Ind. Electron. (ISIE)*, Hangzhou, China, May 2012, pp. 1640–1645.
[11] H. Zhang, F. Mollet, C. Saudemont, and B. Robyns, "Experimental validation of energy storage system management strategies for a local DC distribution system of more electric aircraft," *IEEE Trans. Ind. Electron.*, vol. 57, no. 12, pp. 3905–3916, Dec. 2010.
[12] W. Li, X. Mou, Y. Zhou, and C. Marnay, "On voltage standards for DC home microgrids energized by distributed sources," in *Proc. 7th Int. Power Electron. Motion Control Conf. (IPEMC)*, vol. 3. Harbin, China, Jun. 2012, pp. 2282–2286.
[13] D. McMenamin, "Case studies supporting -48 VDC as the power input of choice for computer equipment deployed in the telecom network," in *Proc. 20th Int. Telecommun. Energy Conf. (INTELEC)*, San Francisco, CA, USA, 1998, pp. 261–265.
[14] R. White, "Computers in the central office-a primer on powering equipment from -48 v," in *Proc. 13th Annu. Conf. Appl. Power Electron. Conf. Expo. (APEC)*, vol. 2. 1998, pp. 902–908.
[15] J. Vasquez, J. Guerrero, J. Miret, M. Castilla, and L. de Vicuna, "Hierarchical control of intelligent microgrids," *IEEE Ind. Electron. Mag.*, vol. 4, no. 4, pp. 23–29, Dec. 2010.
[16] K. Sun, L. Zhang, Y. Xing, and J. Guerrero, "A distributed control strategy based on DC bus signaling for modular photovoltaic generation systems with battery energy storage," *IEEE Trans. Power Electron.*, vol. 26, no. 10, pp. 3032–3045, Oct. 2011.
[17] N. Diaz, A. Luna, and O. Duarte, "Improved MPPT short-circuit current method by a fuzzy short-circuit current estimator," in *Proc. IEEE Energy Convers. Congr. Expo. (ECCE)*, Phoenix, AZ, USA, 2011, pp. 211–218.
[18] Y. Errami, M. Maaroufi, M. Cherkaoui, and M. Ouassaid, "Maximum power point tracking strategy and direct torque control of permanent magnet synchronous generator wind farm," in *Proc. Int. Conf. Complex Syst. (ICCS)*, 2012, pp. 1–6.
[19] R. Majumder, "Some aspects of stability in microgrids," *IEEE Trans. Power Syst.*, vol. 28, no. 3, pp. 3243–3252, Aug. 2013.
[20] A. Kwasinski and C. Onwuchekwa, "Dynamic behavior and stabilization of DC microgrids with instantaneous constant-power loads," *IEEE Trans. Power Electron.*, vol. 26, no. 3, pp. 822–834, Mar. 2011.
[21] D. Linden and T. Reddy, *Handbook of Batteries*. New York, NY, USA: McGraw-Hill, 2002.
[22] A. Rahimi and A. Emadi, "Active damping in DC/DC power electronic converters: A novel method to overcome the problems of constant power loads," *IEEE Trans. Ind. Electron.*, vol. 56, no. 5, pp. 1428–1439, May 2009.
[23] J. Guerrero, J. Vasquez, J. Matas, L. de Vicuña, and M. Castilla, "Hierarchical control of droop-controlled AC and DC microgrids a general approach toward standardization," *IEEE Trans. Ind. Electron.*, vol. 58, no. 1, pp. 158–172, Jan. 2011.
[24] R. Babuska, "Fuzzy and neural control DISC course lecture notes," Delft University of Technology, Sep. 2004.

**Nelson L. Diaz** received the B.S degree in electronic engineering from the Universidad Distrital, Cundinamarca, Colombia, and the M.S. degree in industrial automation from the Universidad Nacional de Colombia, Cundinamarca. He is currently pursuing the Ph.D. degree from the Department of Energy Technology, Aalborg University, Aalborg, Denmark.

He is member of the Research Laboratory of Alternative Energy Sources, Universidad Distrital and Microgrid Research Group, Aalborg University. His current research interests include microgrids and power converters control.

**Tomislav Dragičević** (S'09–M'13) received the M.E.E. and Ph.D. degrees from the Faculty of Electrical Engineering, Zagreb, Croatia, in 2009 and 2013, respectively.

Since 2010, he has been actively cooperating in an industrial project related to design of electrical power supply for remote telecommunication stations. Since 2013, he has been a Full-Time Post-Doctoral at Aalborg University, Aalborg, Denmark. His current research interests include modeling, control, and energy management of intelligent electric vehicle charging stations and other types of microgrids based on renewable energy sources and energy storage technologies.

**Juan C. Vasquez** (M'12) received the B.S. degree in electronics engineering from the Autonoma University of Manizales, Manizales, Colombia, in 2004. He received the Ph.D. degree from the Department of Automatic Control Systems and Computer Engineering, Technical University of Catalonia, Barcelona, Spain, in 2009.

He was a Post-Doctoral Assistant with the Technical University of Catalonia and was also teaching courses based on renewable energy systems. He is currently an Assistant Professor with Aalborg University, Aalborg, Denmark. His current research interests include modeling, simulation, networked control systems, and optimization for power management systems applied to distributed generation in ac/dc microgrids.

**Josep M. Guerrero** (S'01–M'04–SM'08) received the B.S. degree in telecommunications engineering, the M.S. degree in electronics engineering, and the Ph.D. degree in power electronics from the Technical University of Catalonia, Barcelona, Spain, in 1997, 2000, and 2003, respectively.

Since 2011, he has been a Full Professor with the Department of Energy Technology, Aalborg University, Aalborg, Denmark, where he is responsible for the Microgrid Research Program. Since 2012, he has been a Guest Professor at the Chinese Academy of Science, Beijing, China, and the Nanjing University of Aeronautics and Astronautics, Nanjing, China. Since 2014, he has been a Chair Professor with Shandong University, Jinan, China. His current research interests include oriented to different microgrid aspects, power electronics, distributed energy-storage systems, hierarchical and cooperative control, energy management systems, and optimization of microgrids and islanded minigrids.

Prof. Guerrero is an Associate Editor for the IEEE TRANSACTIONS ON POWER ELECTRONICS, the IEEE TRANSACTIONS ON INDUSTRIAL ELECTRONICS, and the IEEE INDUSTRIAL ELECTRONICS MAGAZINE, and an Editor for the IEEE TRANSACTIONS ON SMART GRID. He has been Guest Editor of the IEEE TRANSACTIONS ON POWER ELECTRONICS Special Issues: Power Electronics for Wind Energy Conversion and Power Electronics for Microgrids; the IEEE TRANSACTIONS ON INDUSTRIAL ELECTRONICS Special Sections: Uninterruptible Power Supplies Systems, Renewable Energy Systems, Distributed Generation, and Microgrids, and Industrial Applications and Implementation Issues of the Kalman Filter; and the IEEE TRANSACTIONS ON SMART GRID Special Issue on Smart DC Distribution Systems. He was the Chair of the Renewable Energy Systems Technical Committee of the IEEE Industrial Electronics Society. In 2014, he was awarded by Thomson Reuters as a Highly Cited Researcher.